GIMC structure based Anti-Windup control considering L2 performance

メタデータ	
	言語: eng
	出版者:
	公開日: 2017-10-03
	キーワード (Ja):
	キーワード (En):
	作成者:
	メールアドレス:
	所属:
URL	http://hdl.handle.net/2297/21675

GIMC Structure based Anti-Windup Control Considering $\mathcal{L}_2$ Performance

Yusuke Nakashima and Toru Namerikawa

Abstract— This paper deals with GIMC (Generalized Internal Model Control) structure based Anti-Windup (AW) control system design. First, we setup a $\mathcal{L}_2$ performance criterion based on GIMC structure for Anti-Windup control problems. The design problem is formulated as an optimization problem with a parameter Q. Then we calculate the optimization problem and find an optimal Q. Finally, the effectiveness of proposed method is shown by experimental results for a magnetic suspension system.

I. INTRODUCTION

Recent years, the switching control has been actively researched under increasingly complex conditions of electrical and mechanical systems. The merit of switching control is known as a flexible acceptability for various situation of control systems, e.g., robustness for model parameter variations and faults, etc.

As one of the switching control, there exists GIMC (Generalized Internal Model Control) structure, and it has attracted researcher's attention in area of Fault Tolerant Control [1]. GIMC structure can achieve both performance and robustness specifications based on a switching strategy: a nominal high performance controller K_0 controls the nominal plant and a robust controller K maintains stability for perturbed plants. The effectiveness of GIMC was verified by using an unstable plant in [2]. Moreover, GIMC has been applied to a plant with large time delays by using the Smith Predictor [3]. These research works have shown that the GIMC is very useful for system perturbations.

By the way, in many practical control systems, there exists saturation and constraints on control inputs. The input signals might be greatly saturated when a controller is designed disregarding an input saturation for such a system. The performance may be remarkably deteriorated or the plant might be unstabilized occasionally. Such a phenomenon is known as "windup". The purpose of an Anti-Windup control is to achieve good control performance even in the presence of input saturations.

In this paper, we treat an input saturation problem as a kind of nonlinear perturbation of the system, and design Anti-Windup controller by using GIMC structure. There has been many design methods of AW controller [4]-[11]. Among them, Teel et al.[5] proposed a $\mathcal{L}_2$ performance criterion from the difference between the input signal generated in the closed-loop without input saturation and the signal passed

Y. Nakashima is with Division of Electrical Engineering and Computer Science, Kanazawa University, Kakuma, Kanazawa 920-1192, JAPAN. T. Namerikawa is with Department of System Design Engineering, Keio University, 3-14-1 Hiyoshi, Kohoku-ku, Yokohama 223-8522 JAPAN. `namerikawa@sd.keio.ac.jp`

through the nonlinear saturation to the error of plant outputs. It guarantees performance as well as the stability for input saturations. A systematic design method by using the $\mathcal{L}_2$ performance criterion has been proposed by [7]. However it has been well-known that it was impossible to obtain a bounded feedback control law that achieves global output regulation in the case the plant has unstable poles. Furthermore this design method only considers a global stability.

Moreover, an Anti-Windup control based on Youla parametrization has been proposed by Takaba[8]. In [8], he proposed a direct design method and an AW controller which achieved the prescribed quadratic performance bound. In this technique, a good performance and stability achieves when a reference signal or limit of saturation are invariable. If these parameter values would change, however, the performance and the stability can not be guaranteed. Gain-Scheduling control has been also actively researched in recent years[11] and Wada et al proposed a controller which is composed of a gain-scheduled feedback control law and a standard observer in [11]. The scheduling parameter is computed in the real time by solving a convex optimization problem based on the information of the state variables estimated by the observer. The GIMC structure can switch the control configuration by an internal signal, therefore it has a simpler structure and a less burden for calculation than gain scheduling control method. Hence it is more useful in practice.

Our goal is to apply GIMC structure to Anti-Windup control problem and construct switching Anti-Windup controller considering $\mathcal{L}_2$ performance criterion. First, we setup a $\mathcal{L}_2$ performance criterion based on GIMC structure for Anti-Windup control problems. The design problem is formulated as an optimization problem with a parameter Q. Then we calculate the optimization problem and find an optimal Q. Finally, the effectiveness of proposed method is shown by experimental results for a magnetic suspension system.

II. PROBLEM STATEMENT

In this section, we firstly describe the definition of GIMC structure and Anti-Windup control system, and we also define the saturation and deadzone functions. Then we setup a $\mathcal{L}_2$ performance criterion based on GIMC structure for Anti-Windup control problems in the next section.

A. GIMC Structure

The configuration of the GIMC structure is shown in Fig. 1. Let $P(s)$ be a nominal model of the real physical plant $\tilde{P}(s)$ and $K_0(s)$ be a stabilizing controller for $P(s)$. In addition, it should be noted that $\tilde{M}(s), \tilde{N}(s)$ are left coprime

factorization of the model $P(s)$ and $\tilde{V}(s)$, $\tilde{U}(s)$ are also left coprime factorization of the controller $K_0(s)$. They have the following state-space realizations:

$$\tilde{P} = \left[\begin{array}{c|c} A_p & B_p \\ \hline C_p & D_p \end{array} \right], \quad K_0 = \left[\begin{array}{c|c} A_k & B_k \\ \hline C_k & D_k \end{array} \right] \tag{1}$$

$$\left[\begin{array}{cc} \tilde{N} & \tilde{M} \end{array} \right] = \left[\begin{array}{c|cc} A_p + L_p C_p & B_p + L_p D_p & L_p \\ \hline C_p & D_p & I \end{array} \right] \tag{2}$$

$$\left[\begin{array}{cc} \tilde{U} & \tilde{V} \end{array} \right] = \left[\begin{array}{c|cc} A_k + L_k C_k & B_k + L_k D_k & L_k \\ \hline C_k & D_k & I \end{array} \right] \tag{3}$$

$$\tilde{M}, \tilde{N}, \tilde{V}, \tilde{U} \quad \in \quad \mathcal{RH}_\infty \tag{4}$$

Where $A_p + L_p C_p$ and $A_k + L_k C_k$ are stable. If there are no disagreement between P and $\tilde{P}$ nor exogenous disturbances, then $z = 0$. The control system is controlled by K_0. If there exists either model uncertainties, disturbance or faults, however, the inner loop can be activated because $z \neq 0$. The entire feedback system is controlled by

$$K(s) = (\tilde{V} - Q\tilde{N})^{-1}(\tilde{U} + Q\tilde{M}) \tag{5}$$
$$det(\tilde{V} - Q\tilde{N})(\infty) \neq 0, \quad Q \in \mathcal{RH}_\infty \tag{6}$$

GIMC structure can switch two controllers which are $K_0(s)$ and $K(s)$ by using the internal signal $z(s)$ in the above way. In this paper, we treat an input saturation as a perturbation of control input, and a bad influence of the saturation should be kept to the minimum by switching controllers when the saturation occurs. Hence we treat the saturation as a perturbation and the closed-loop system can be transformed from Fig. 1 into Fig. 2. Here we assume there should be no error between the model and the plant as the following.
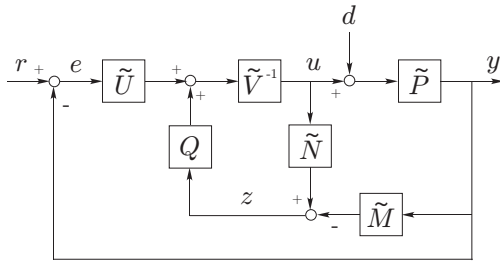
$$\tilde{P} = P \tag{7}$$

Fig. 1.   GIMC Structure

B. Saturation and Deadzone

The saturation nonlinearity Φ_f and the deadzone nonlinearity Ψ_f are defined as

$$\Phi_f(u) = \left\{ \begin{array}{ccl} f & if & u > f \\ u & if & -f < u < f \\ -f & if & -f > u \end{array} \right. \tag{8}$$

$$\Psi_f(u) = \left\{ \begin{array}{ccl} u - f & if & u > f \\ 0 & if & -f < u < f \\ u + f & if & -f > u \end{array} \right. \tag{9}$$
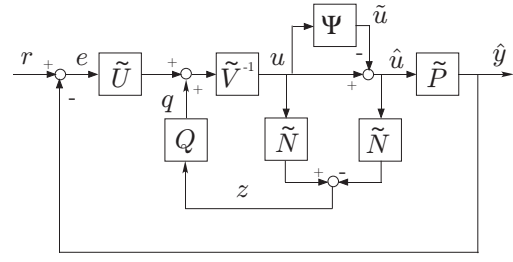
$$\Psi_f(u) = u - \Phi_f(u) \tag{10}$$

Fig. 2.   GIMC Structure with Deadzone

In case of $f = 1$, then the subscript f is dropped. Given a diagonal matrix $F = diag(f_1, \cdots, f_n)$ with $f_i > 0$ for each $i \in \{1, 2, \cdots, n\}$, we denote $\Phi_F : \mathbb{R}^n \to \mathbb{R}^n$ and $\Psi_F : \mathbb{R}^n \to \mathbb{R}^n$ as the component-wise multivariable saturation and deadzone functions as the followings,

$$\Phi_F(u) = (\Phi_{f1}(u_1), \cdots, \Phi_{fn}(u_n))^T \tag{11}$$
$$\Psi_F(u) = (\Psi_{f1}(u_1), \cdots, \Psi_{fn}(u_n))^T \tag{12}$$

and if $F = I$, then we drop the subscript. Here we assume Ψ_{f_i} in the sector $[0, c]$ $(0 < c < 1)$.

$$0 \leq \frac{\Psi_{f_i}(u_i)}{u_i} \leq c, \quad \forall u \neq 0, \quad \Psi_{f_i}(0) = 0 \tag{13}$$
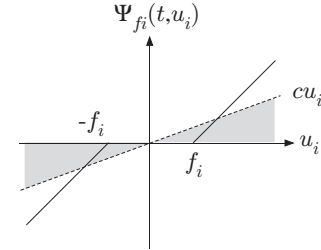

Fig. 3.   Deadzone and Sector Bounded

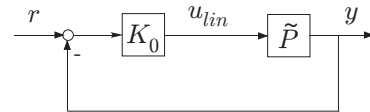## III. ANTI-WINDUP CONTROL CONSIDERING $\mathcal{L}_2$ PERFORMANCE

Fig. 4.   Nominal Linear System

In this section, we setup a $\mathcal{L}_2$ performance criterion based on GIMC structure for Anti-Windup control problems in the next section. Then we derive the condition which is based on Youla parametrization Q.

From Fig. 2 and Fig. 4, input and output error signals between the nominal linear system and the Anti-Windup control system are written as follows:

$$\hat{y} - y = -P(G + I)\tilde{u} \tag{14}$$
$$u - u_{lin} = -G\tilde{u} \tag{15}$$

where

$$G = -(I + PK_0)^{-1}(PK_0 + \tilde{V}^{-1}Q\tilde{N}) \quad (16)$$

Here we consider the following design problem.

Problem 1 Select the parameter $Q(s) \in \mathcal{RH}_\infty$ which minimizes the $\mathcal{L}_2$ gain γ concerning equations (14), (16).

$$||\hat{y} - y||_{\mathcal{L}_2} \le \gamma \Psi(u_{lin}) \quad (17)$$

Here, we introduce the following lemma for the deadzone function Ψ_F .

Lemma 1 For any $F = diag(f_1, \cdots, f_n) > 0$ and any $x, y \in \mathbb{R}^n$ and $\Psi_F(x), y \in \mathcal{L}_{2[0,T)}$, the following relation achieves.

$$||\Psi_F(x + y)||_{\mathcal{L}_{2[0,T)}} \le ||\Psi_F(x)||_{\mathcal{L}_{2[0,T)}} + ||y||_{\mathcal{L}_{2[0,T)}} \quad (18)$$

Using this lemma, the following theorem is approved.

Theorem 1 We assume that Q exists with any $F = diag(f_1, \cdots, f_n), f_i > 0$ and any $K = diag(k_1, \cdots, k_n), 0 < k_i < 1$ such that

$$||F(G + I) - K||_\infty < 1 \quad (19)$$

Furthermore, γ is given as follows with $\Psi(u_{lin}) \in \mathcal{L}_2$

$$\gamma = \frac{||F|| \, ||P(G + I)||_\infty}{1 - ||F(G + I) - K||_\infty} \quad (20)$$

Proof: Fig. 5 is the system which expresses (15) by a block diagram, and it is equivalent in point of stability with Fig. 2. Consider the system in Fig. 6, which is equivalent to Fig. 5. From Fig. 6, lemma 1 and (19), we can get the following inequality.

$$||\tilde{u}||_{\mathcal{L}_2[0,T)} \le$$
$$\frac{||F||}{1 - ||F(G + I) - K||_\infty} ||\Psi(u_{lin})||_{\mathcal{L}_2[0,T)} \quad (21)$$

In addition, from (14)

$$||\hat{y} - y||_{\mathcal{L}_{2[0,T)}} = || - P(G + I)\tilde{u}||_{\mathcal{L}_{2[0,T)}} \quad (22)$$
$$\le ||P(G + I)||_\infty ||\tilde{u}||_{\mathcal{L}_{2[0,T)}} \quad (23)$$

We can conclude from (21) and (23) as follows.

$$||\hat{y} - y||_{\mathcal{L}_2} \le \frac{||F|| \, ||P(G + I)||_\infty}{1 - ||F(G + I) - K||_\infty} ||\Psi(u_{lin})||_{\mathcal{L}_2}$$
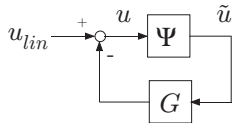$$= \gamma ||\Psi(u_{lin})||_{\mathcal{L}_2}$$

∎

Fig. 5.   System for Close Loop Stability

Remark 1 Note that (19) is the condition of stability for input saturation. In scalar case, (19) is represented by the following inequality.
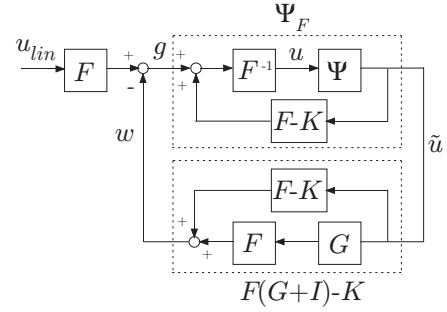
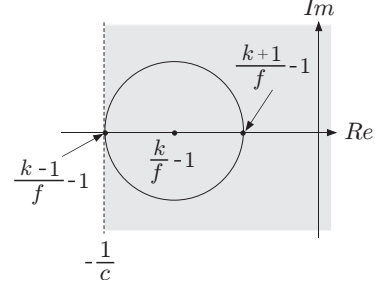$$|f(G + 1) - k| < 1 \quad (24)$$

Fig. 6.   Equivalent System

Fig. 7.   Constraint Condition and Stability Region

Here, we put $G = \alpha + j\beta$ then

$$\left(\alpha + 1 - \frac{k}{f}\right)^2 + \beta^2 < \left(\frac{1}{f}\right)^2 \quad (25)$$

The Nyquist plot of G remains in the circle of Fig. 7. Furthermore, from circle criterion [12], Fig. 5 is $\mathcal{L}_2$ stable for the sector $[0, c]$ when G is Hurwitz and the Nyquist plot of G lies to the right of the vertical line defined by $Re[s] = -\frac{1}{c}$ represent in Fig. 7. To put it the other way around, it is possible to design in consideration of local stability using the following relation.

$$c = \frac{f}{f + 1 - k} \quad (26)$$

Where, c and γ have the following relations from (20) and (26).

$$\gamma = \frac{|P(G + 1)|}{1 - |f(G + \frac{1}{c}) - 1|} \quad (27)$$

It shows if c becomes larger, γ grows, too. That is, there exists a relation of the trade-off between performance and stability. **Remark 2** Above trade-off can be solved by switching strategy of Fig. 8. In this paper, we switch Q_1 and Q_2 by using internal signal z. If z is bigger than a threshold then we use robust controller Q_2, and other we use high performance controller Q_1.

IV. CONTROL DESIGN

A. Control Object and Nominal Controller

The controlled plant $\tilde{P}(s)$ in this research is a magnetic suspension system shown in Fig. 9. A transfer function of plant model $P(s)$ is given as (28). Where, the model
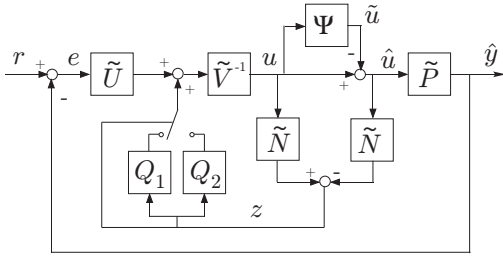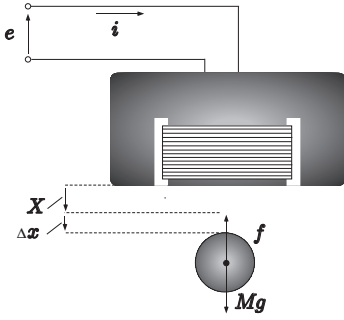
Fig. 8. AW Control with Switching

Fig. 9. Magnetic Suspension System

Parameter	Value
Mass of iron boll M[kg]	0.286
Stedy gap X[m]	3.00×10^{-3}
Correction term x_0[m]	5.014×10^{-3}
Coefficient k[Nm^2/A^2]	2.35×10^{-4}
Inductance of Electromagnetic L[H]	0.319
Resistance of Electromagnetic R [Ω]	9.7716
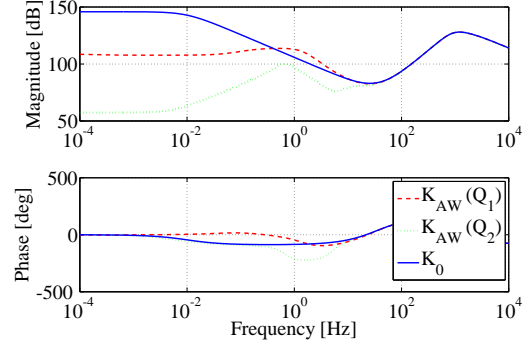
Fig. 10. Bode Diagram of Controllers

parameters are shown in Table I. $P(s)$ is an unstable system as shown in (28).

$$P(s) = -\frac{k_i}{(Ms^2 - k_x)(Ls + R)} \quad (28)$$

$$= -\frac{69.9}{(s + 49.2)(s + 30.6)(s - 49.2)} \quad (29)$$

$$k_x = \frac{2kI^2}{(X + x_0)^3}, \quad k_i = \frac{2kI}{(X + x_0)^2} \quad (30)$$

A nominal controller K_0 which achieves stabilizing and desirable performance for the plant is designed by $\mathcal{H}_\infty$ control theory. A transfer function of $K_0(s)$ is given as (31). The frequency response of K_0 is shown in Fig. 10.

$$K_0 = \frac{(s + 49.2)(s + 30.6)(s + 33.1)}{(s + 570.4 + j717.2)(s + 570.4 - j717.2)} \quad (31)$$
$$\times \frac{1}{(s + 1549.3)(s + 0.01)}$$

B. Left Coprime Factorization

The left coprime factorizations of $P(s)$ and $K_0(s)$ are shown in (2) and (3). Because (C, A) and (C_k, A_k) are observable, we can decide the left coprime factorization by the pole placement. Here we decide the eigenvalues in (32) and (33).

$$\lambda(A_p + L_pC_p) = \{-200, -190, -180\} \quad (32)$$
$$\lambda(A_k + L_kC_k) = \{-2000, -710, -700, -100\} \quad (33)$$

C. Anti-Windup Controller Design

AW controller is represented by using Q-parametrization as follows.

$$K_{AW}(s) = (\tilde{V} - Q\tilde{N})^{-1}(\tilde{U} + Q\tilde{M}) \quad (34)$$
$$det(\tilde{V} - Q\tilde{N})(\infty) \neq 0 \quad (35)$$

Q is calculated by optimization calculation of Simplex and Simple GA method based on (20). We fix the order of Q as 3/4. The design parameters and γ and c are shown in Table II. Here, parametorization Q_1, Q_2 whose c are different are obtained by changing the design parameters K. From Table II, Q_1 seems to have better performance but its stability should be worse because γ and c are relatively lower. On the other hands, Q_2 seems to have better stability but its performance is worse. The transfer function of Q_1 and Q_2 are also shown in (36) and (37).

$$Q_1 = \frac{(s + 0.4)(s + 0.2)(s + 2.2 \times 10^{-4})}{(s + 39)(s + 5.6)(s + 6.6 \times 10^{-2})(s + 2.4 \times 10^{-4})} \quad (36)$$

$$Q_2 = \frac{(s + 6.7 \times 10^{-2})(s + 0.2 - j0.6)(s + 0.2 + j0.6)}{(s + 2.6 \times 10^{-3})(s + 2.5 + j4.8)(s + 2.5 - j4.8)}$$
$$\times \frac{1}{(s + 6.9 \times 10^{-2})} \quad (37)$$

The frequency responses of controllers $K_{AW}(Q_1)$ and $K_{AW}(Q_2)$ are shown in Fig. 10. From this figure, we can see that the lower frequency Gain of $K_{AW}(Q_1)$ and $K_{AW}(Q_2)$ is lower than that of the nominal controller K_0. It may cause the decreasing of integral action. And the input may return to nominal more quickly. Compared the controller of $K_{AW}(Q_1)$ with $K_{AW}(Q_2)$, from low to middle frequency gain of $K_{AW}(Q_2)$ is lower than that of $K_{AW}(Q_1)$. It may cause servility performance degradation of $K_{AW}(Q_2)$.

TABLE II

CALCULATE RESULT

Q	γ	c	F	K
Q_1	2.6×10^{-5}	0.22	0.028	0.9
Q_2	0.39	0.74	0.028	0.99

V. EXPERIMENTAL RESULTS

In this section, we show the effectiveness of the proposed method. At first, we compare the performance of $K_{AW}(Q_1)$ with $K_{AW}(Q_2)$. Next, we try to switching control by using $K_{AW}(Q_1)$ and $K_{AW}(Q_2)$.

A. Verification of $\mathcal{L}_2$ Performance

We evaluate the step response by using MSS. The step reference signal is 1[mm] under from the steady gap. Also, we set the saturation virtually on the computer and the saturation limit is ± 5.5[V]. Experimental results are shown in Fig. 11-14. Where Fig. 11 and Fig. 13 are output, FIg. 12 an Fig. 14 are input. Fig. 11 and Fig. 13 show that AW responses are better transient response than no AW responses and we can confirm the effect of AW control for unstable system. Also, these figures show that the performance of $K_{AW}(Q_1)$ which has small γ is better than that of $K_{AW}(Q_2)$ which has large γ. Next, experimental results which the step reference signal switch from 1[mm] to 1.1[mm] are shown in Fig. 15-18. Fig. 15 show that the resopnse of $K_{AW}(Q_1)$ which has small c become unstable. On the other hand, Fig. 17 show that the resopnse of $K_{AW}(Q_2)$ which has large c is stable. From above, we can confirm the trade-off between performance with stability.

B. Switching control experiments

Switching control experimental results are shown in Fig. 19-20. Where, the step reference signal is 1.1[mm] and the saturation limit is ± 5.5[V]. Also, the threshold value for the switching is $|z| = 1 \times 10^{-4}$ shown in Fig. 20. As we showed in Fig. 15 and Fig. 17, the resopnse of $K_{AW}(Q_1)$ become unstable and the resopnse of $K_{AW}(Q_2)$ is converge with reference taking a long time. But the switching response shown in Fig. 19 is stable and converge quickly. Therefore, we can achieve a good balance between performance and stability.

VI. CONCLUSION

In this paper, we have proposed GIMC based Anti-Windup control. By experimental results, we can achieve the good performance when an input is saturate, and we see it can design AW controller by using GIMC structure. Also, we have proposed AW switching control by using high performance Q_1 and robust Q_2. The proposed switching method is effective on the special situation which is not able to supported by conventional unitary controller, for example the reference signal or saturation limits may vary. Furthermore, proposed method is more simple and less calculation amount than gain scheduling method.

REFERENCES

[1] Kemin Zhou, "A Natural Approach to High Performance Robust Control: Another Look at Youla Parameterization," *Proc. in SICE Annual Conference*, pp. 869-874, 2004.

[2] T. Namerikawa and H. Maruyama, "High Performance Robust Control of Magnetic Suspension System Using GIMC Structure," *Proc. in American Control Conference*, 2006.

[3] T. Namerikawa and J. Miyakawa, "GIMC Structure Considering Communication Delay and Its Application to Mechatronic System," *Proc. in American Control Conference*, 2007.

[4] A. Zheng, M. V. Kothare and M. Morari, "Anti-Windup design for internal model control," *Int. Jounal of Control*, **60**-5, pp. 1015-1024, 1994.

[5] A. R. Teel and N. Kapoor, "The $\mathcal{L}_2$ anti-windup problem:It's definition and solution," *Proc. in European Control Conference*, 1997.

[6] A. R. Teel, "Anti-Windup for exponentially unstable linear systems," *International Journal of Robust and Nonlinear Control*, **9**, pp. 701-716, 1999.

[7] S. Crawshaw and G. Vinnicombe, "Anti-windup synthesis for guaranteed $\mathcal{L}_2$ performance," *Proc. in IEEE Conference on Decision Control*, 2000.

[8] Kiyotsugu Takaba, "Anti-Windup Control System Design Based on Youla Parametrization," *Proc. in American Control Conference*, 1999.

[9] C. Edwards and I. Postlethwaite, "An anti-windup scheme with closed-loop stability considerations," *Automatica*, **35**, pp. 761-765, 1999.

[10] Matthew C. Turner, Guido Herrmann and Ian Postlethwaite, "Incorporating Robustness Requirements Into Antiwindup Design," *Automatic Control*, **52**-10, pp. 1842-1853, 2007.

[11] N. Wada and M. Saeki, "An LMI Based Scheduling Algorithm for Constrained Stabilization Problem," *Proc. 49th Japan Joint Automatic Control Conference*, 2006.

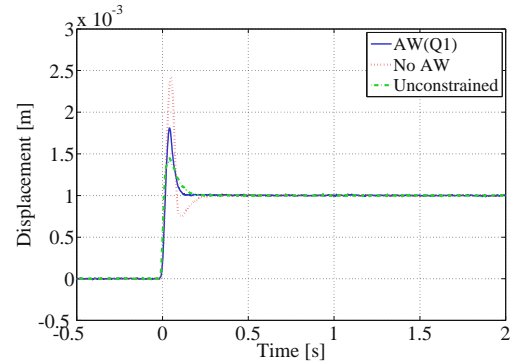[12] Hassan K. Khalil, Nonlinear System, Prentice-Hall, 1996.
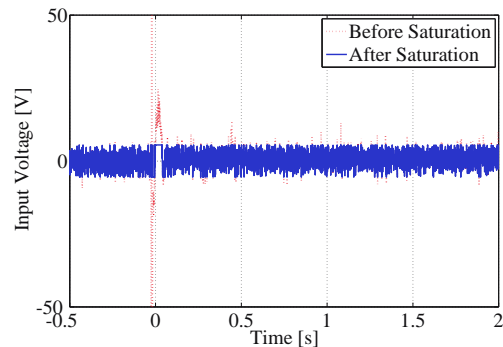

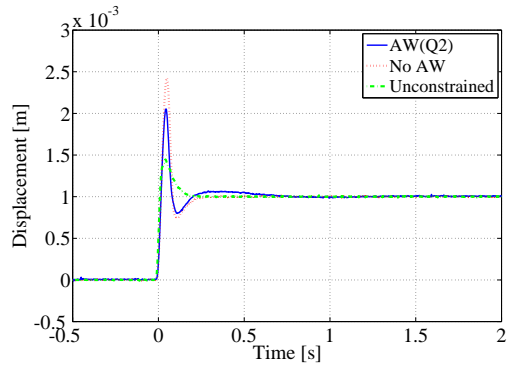Fig. 11.   Step Responses (AW Q_1)

Fig. 12.   Control Input (AW Q_1)
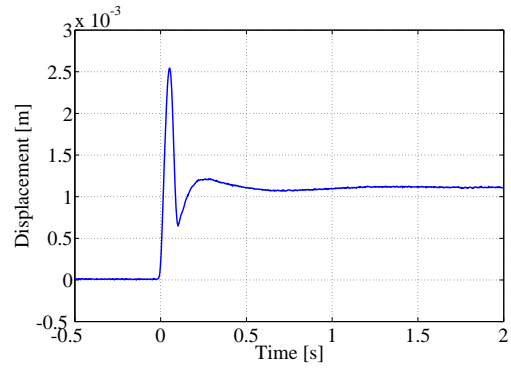
Fig. 13.   Step Responses (AW Q_2)

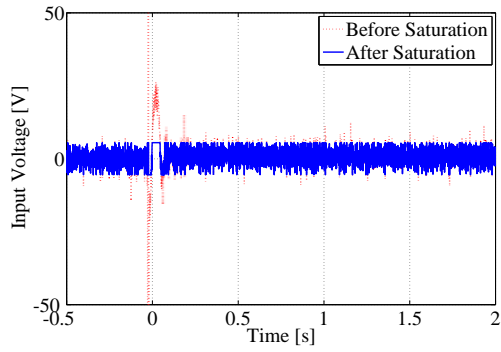Fig. 17.   Step Response (AW Q_2)

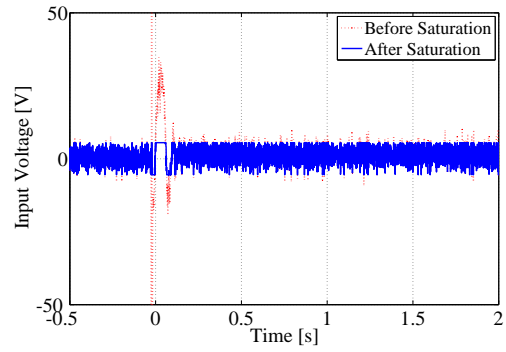Fig. 14.   Control Input (AW Q_2)
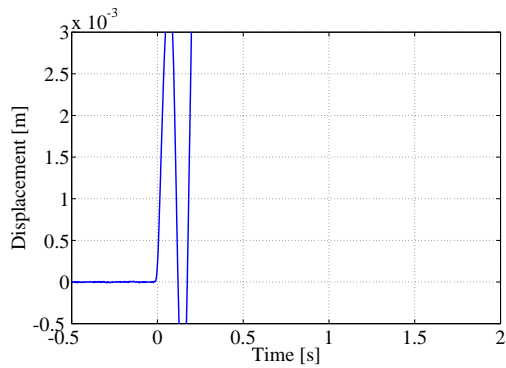

Fig. 18.   Control Input (AW Q_2)

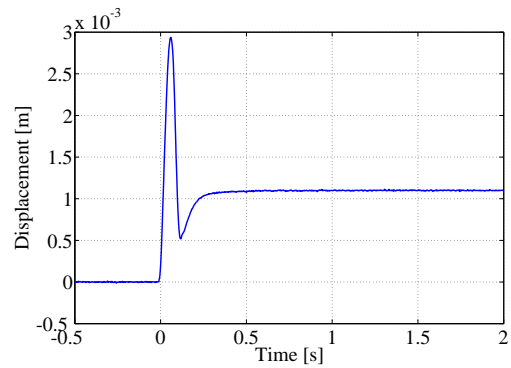Fig. 15.   Step Response (AW Q_1)

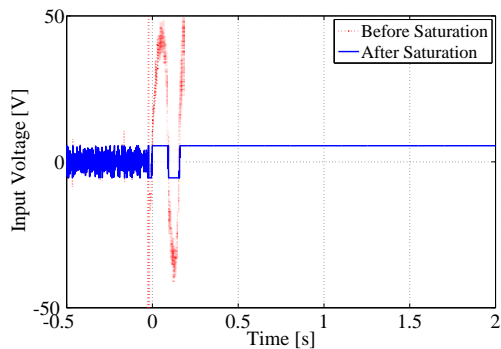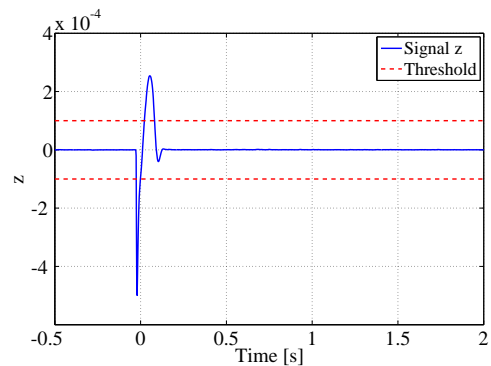Fig. 19.   Step Response (AW with Switching)

Fig. 16.   Control Input (AW Q_1)

Fig. 20.   Internal Signal z(AW with Switching)